

## OH in the tropical upper troposphere and its relationships to solar radiation and reactive nitrogen

R. S. Gao · K. H. Rosenlof · D. W. Fahey ·  
P. O. Wennberg · E. J. Hints · T. F. Hanisco

Received: 13 August 2013 / Accepted: 23 March 2014 /  
Published online: 12 April 2014  
© Springer Science+Business Media Dordrecht 2014

**Abstract** In situ measurements of [OH], [HO<sub>2</sub>] (square brackets denote species concentrations), and other chemical species were made in the tropical upper troposphere (TUT). [OH] showed a robust correlation with solar zenith angle. Beyond this dependence, however, [OH] did not correlate to its primary source, the product of [O<sub>3</sub>] and [H<sub>2</sub>O] ([O<sub>3</sub>]•[H<sub>2</sub>O]), or its sink [NO<sub>y</sub>]. This suggests that [OH] is heavily buffered in the TUT. One important exception to this result is found in regions with very low [O<sub>3</sub>], [NO], and [NO<sub>y</sub>]. Under these conditions, [OH] is highly suppressed, pointing to the critical role of NO in sustaining OH in the TUT and the possibility of low [OH] over the western Pacific warm pool due to strong marine convections bringing NO-poor air to the TUT. In contrast to [OH], [HO<sub>x</sub>] ([OH] + [HO<sub>2</sub>]) correlated reasonably well with [O<sub>3</sub>]•[H<sub>2</sub>O]/[NO<sub>y</sub>], suggesting that [O<sub>3</sub>]•[H<sub>2</sub>O] and [NO<sub>y</sub>] are the significant source and sink, respectively, of [HO<sub>x</sub>].

**Keywords** OH · In situ · Tropical upper troposphere · STRAT

R. S. Gao (✉) · K. H. Rosenlof · D. W. Fahey  
Chemical Sciences Division, Earth System Research Laboratory, National Oceanic and Atmospheric Administration, Boulder, CO 80305, USA  
e-mail: RuShan.Gao@noaa.gov

D. W. Fahey · E. J. Hints  
Cooperative Institute for Research in Environmental Sciences, University of Colorado,  
Boulder, CO 80309, USA

P. O. Wennberg  
Divisions of Geological and Planetary Sciences and Engineering and Applied Science,  
California Institute of Technology, Pasadena, CA 91125, USA

E. J. Hints  
Global Monitoring Division, Earth System Research Laboratory, National Oceanic and Atmospheric Administration, Boulder, CO 80305, USA

T. F. Hanisco  
Goddard Space Flight Center, National Aeronautics and Space Administration, Greenbelt, MD, USA

## 1 Introduction

The hydroxyl radical (OH) is the most important oxidant of a number of short-lived stratospheric ozone-depleting substances in the tropical upper troposphere (TUT) (Brioude et al. 2010). Understanding its distribution in the TUT is thus critical for predicting the ozone depletion potential of these very short-lived substances. The OH distribution in the TUT is also important for controlling the delivery of sulfur to the stratosphere and, thereby, the amount of stratospheric aerosol (Weissenstein et al. 1997; Rae et al. 2007). There are few OH measurements currently available in the tropical upper troposphere, particularly in regions of active troposphere-to-stratosphere exchange.

In the TUT, OH is produced from O<sub>3</sub> and H<sub>2</sub>O photochemical reactions (Kley et al. 1996; Wennberg et al. 1998; Jaeglé et al. 2001):



Due to uplift associated with strong convection, the composition of air in the TUT, particularly in the tropical Pacific region, is greatly affected by near-surface air (Kley et al. 1996; Folkens et al. 2006). As a consequence, O<sub>3</sub> concentrations in the TUT can reach very low levels (<20 ppb) in the Western Pacific warm pool region. Furthermore, TUT H<sub>2</sub>O concentrations over the warm pool are very low due to the very low ambient temperatures (Newell and Gould-Stewart 1981). Since O<sub>3</sub> and H<sub>2</sub>O are source species for OH, low concentrations of these species may lead to low [OH] (square brackets denote species concentrations hereafter) and some model studies appear to support this conjecture (e.g. Kley et al. 1996). Other model studies (Crawford et al. 1999) showed a very weak dependence of OH on [O<sub>3</sub>] and [H<sub>2</sub>O]. This weak dependence was due to a strong HO<sub>x</sub> ([OH] + [HO<sub>2</sub>]) source from autocatalytic production through methane oxidation (Wennberg et al. 1998; Jaeglé et al. 2001).

Observationally, [OH] is found to be largely independent of [O<sub>3</sub>] and [H<sub>2</sub>O] in both the lower stratosphere (LS) (Wennberg et al. 1994b; Hanisco et al. 2001) and free troposphere (Rohrer and Berresheim 2006). In both cases, [OH] values were found to be proportional to ambient photolysis rates; namely, a linear combination of photolysis rates for O(^1D) and CH<sub>2</sub>O in the LS and the photolysis rate for O(^1D) alone in the free troposphere. These proportionalities suggest that either the sinks for OH are correlated with OH sources, or that OH is highly buffered in these regions. We note that the latter is a sufficient (but not necessary) condition for the near constant global OH levels reported by Montzka et al. (2011).

In this study, we show OH measurements from an extended set of high-altitude aircraft flights that provide a unique dataset for examining the role of OH in the TUT. We show that [OH] in the TUT behaves very much the same as [OH] in the lower stratosphere as reported by Hanisco et al. (2001). While the product of [O<sub>3</sub>] and [H<sub>2</sub>O] varies by about 3 orders of magnitude, most [OH] data deviate less than a factor of 2 from a functional fit (a linear combination of photolysis rates for O(^1D) and CH<sub>2</sub>O) of stratospheric [OH] vs. solar zenith angle (SZA) (Hanisco et al. 2001). The largest anomaly from this near-constancy is the association of very low [OH] values with air masses depleted in [NO].

## 2 Measurements

The dataset used for this work was collected using a suite of in situ instruments onboard the NASA ER-2 high-altitude research aircraft during the NASA Stratospheric Tracers of Atmospheric Transport (STRAT) field mission (1995–1996). OH and HO<sub>2</sub> were measured with a laser-induced fluorescence instrument (Wennberg et al. 1994a). O<sub>3</sub> was measured by a dual-beam UV photometer (Proffitt and McLaughlin 1983). A Lyman- $\alpha$  hygrometer was used for H<sub>2</sub>O measurements (Weinstock et al. 1994). Measurements of NO and NO<sub>y</sub> were made with a chemiluminescence detector (Gao et al. 1997). CO was measured using a laser absorption spectrometer (Webster et al. 1994). Temperature and pressure were obtained using the onboard meteorological measurement system (Scott et al. 1990).

Latitudes sampled by ER-2 flight tracks during STRAT ranged from 2°S to 60°N. Flights during STRAT originated either from Moffett Field, CA or Barbers Point Naval Air Station (now Kalaeloa Airport), HI. Only flights based at Barbers Point were used in this work (1 to 23°N). A significant amount of flight time (~76 %) was spent in the lower stratosphere during these flights. Only upper tropospheric data between 9 km and the tropopause with O<sub>3</sub> mixing ratio below 150 parts per billion (ppb) are used for this study. Tropopause heights along the flight tracks were determined using temperature profiles taken by the Microwave Temperature Profiler instrument (Denning et al. 1989).

Both NO and NO<sub>y</sub> are tightly correlated with O<sub>3</sub>, while H<sub>2</sub>O is clearly dependent on ambient temperature (Fig. 1). The NO<sub>y</sub>-O<sub>3</sub> correlation has a slope of 0.005, approximately twice that observed in the tropical LS in this dataset and 1.6 times that seen in the higher-latitude LS (Fahey et al. 1996). The CO mixing ratio spans a relatively small range (70±20 ppb) and is loosely anti-correlated with O<sub>3</sub>. As Fig. 1a and b suggest, NO and NO<sub>y</sub> in this dataset are also highly correlated (slope = 0.41,  $r^2=0.82$ ). [NO<sub>2</sub>] values during daytime (SZA < ~85°) were in a photochemical steady state with [NO] via reactions R3 and R4 (Gao et al. 1997), and were much lower than [NO] values because formation from [NO] via its reaction with ozone is suppressed due to the low [O<sub>3</sub>] and temperature values while photolysis of NO<sub>2</sub> remains efficient:



[NO<sub>x</sub>] ([NO] + [NO<sub>2</sub>]) is essentially the same as [NO] shown in Fig. 1b. Air parcels with very low [O<sub>3</sub>] and [NO<sub>y</sub>] comparable or close to those reported by Kley et al. (1996) (Fig. 1a inset) were encountered. As in Kley et al. (1996), these air parcels likely experienced recent convection and wet removal of water-soluble species prior to sampling. The absence of enhanced NO levels implies that this convection was not accompanied by large amounts of lightning (Skamarock et al. 2003).

## 3 Results and discussion

[OH] and [HO<sub>x</sub>] are shown as functions of SZA in Fig. 2. [HO<sub>2</sub>] is much greater than [OH] and, therefore, is the dominant component of [HO<sub>x</sub>] (Wennberg et al. 1998). In Fig. 2a and b, a

**Fig. 1** NO, NO<sub>y</sub>, H<sub>2</sub>O and CO mixing ratios shown as functions of O<sub>3</sub>. The dataset includes approximately 3,000 points, each of which is a 10-s average corresponding to approximately 2 km of flight track. Latitude, longitude, temperature, and altitude are shown as *color scales* in panels **a**, **b**, **c**, and **d**. Linear fits of NO and NO<sub>y</sub> are shown in panels **a** and **b** as *black lines*

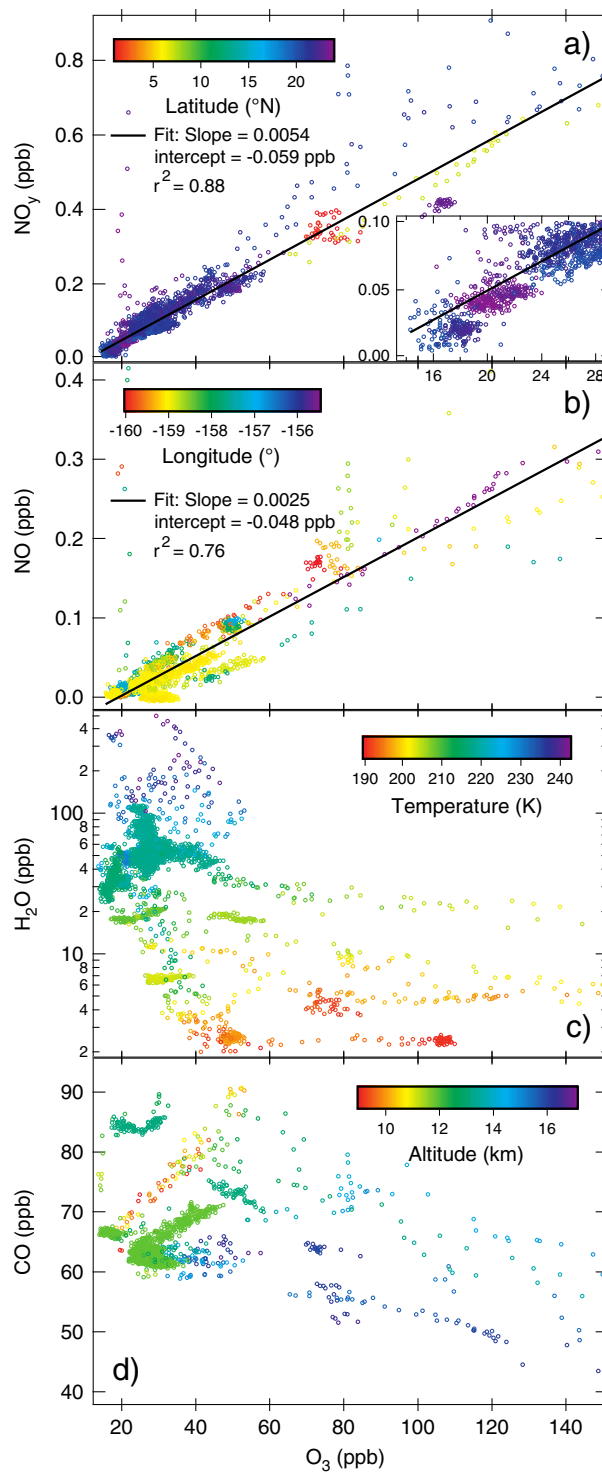
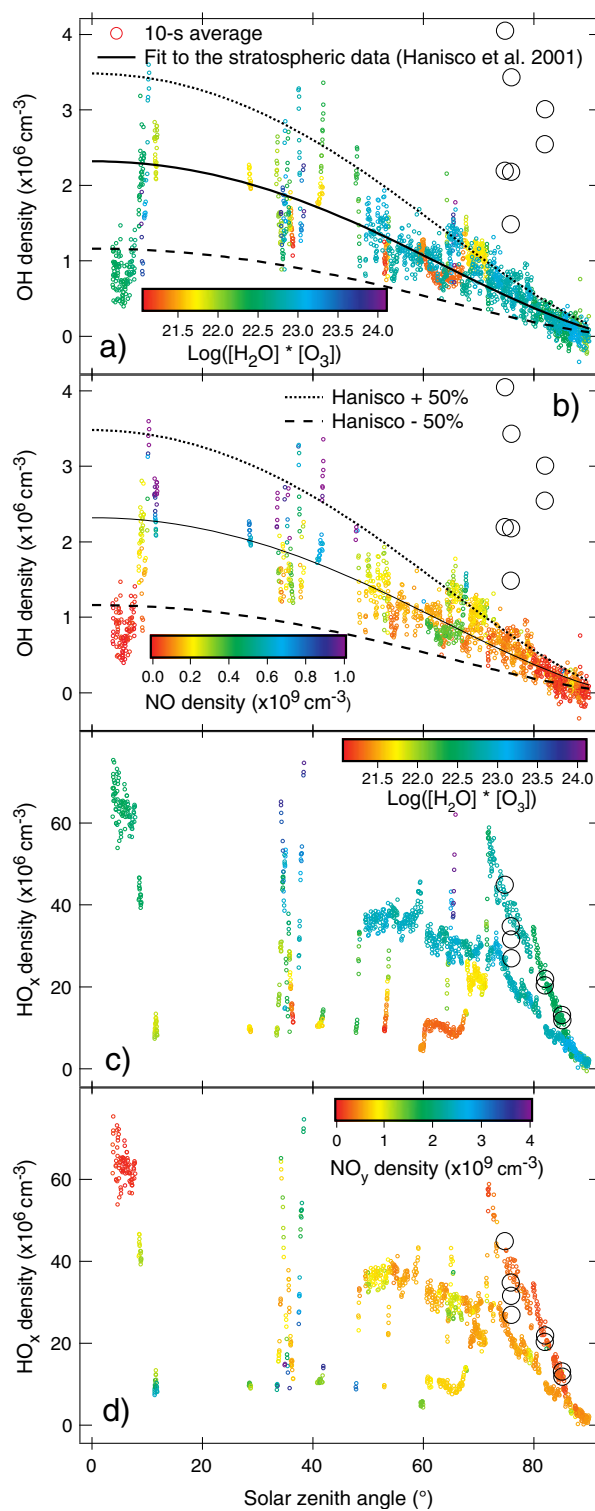


**Fig. 2** [OH] and [HO<sub>x</sub>] shown as functions of solar zenith angle (SZA). The data points correspond to those in Fig. 1. A functional fit to OH concentrations measured in the lower stratosphere (Hanisco et al. 2001) is shown in panels **a** and **b** as the *solid lines*. The *dotted and dashed curves* are the Hanisco fit  $\pm 50\%$  as visual aids



functional fit to [OH] in the lower stratosphere (Hanisco et al. 2001) is shown as the black curve. This fit is expressed as:

$$\begin{aligned} [\text{OH}(\text{SZA})] &= c_1 J_1 + c_2 J_2 \\ J &= J_0 \exp[-\zeta(\sec(\chi)-1)] \\ J_1 : J_0 &= 8 \times 10^{-5}, \zeta = 2.2, \chi = 0.85 \times \text{SZA} \\ J_2 : J_0 &= 6.4 \times 10^{-5}, \zeta = 0.67, \chi = 0.86 \times \text{SZA} \end{aligned} \quad (1)$$

where  $J_0$  is in  $\text{s}^{-1}$ ,  $c_1 = 1.5 \times 10^{10}$  molecules  $\text{cm}^{-3}$  s, and  $c_2 = 1.75 \times 10^{10}$  molecules  $\text{cm}^{-3}$  s.

A few measurements made by the ER-2 while sampling its own exhaust plume (Hanisco et al. 1997) are also shown in Fig. 2 as large black circles (to be discussed below).

The TUT [OH] values in Fig. 2a and b essentially follow the same relationship with respect to SZA as those measured in the lower stratosphere (Hanisco et al. 2001). The primary production rate of OH via reactions R1 and R2 is proportional to the product of  $\text{O}_3$  and  $\text{H}_2\text{O}$  concentrations ( $[\text{O}_3] \cdot [\text{H}_2\text{O}]$ ). In this dataset, where  $[\text{O}_3] \cdot [\text{H}_2\text{O}]$  varies over 3 orders of magnitude, [OH] does not show any correlation to  $[\text{O}_3] \cdot [\text{H}_2\text{O}]$  or  $[\text{NO}_y]$ . The absence of correlation of [OH] to its primary production source (R1 and R2) suggests that low  $[\text{O}_3]$  and  $[\text{H}_2\text{O}]$  do not necessarily lead to low [OH]; consequently the primary production rates alone are insufficient to predict [OH].

The lack of correlation of [OH] to its source gases is not entirely surprising. [OH] and  $[\text{HO}_2]$  are tightly coupled via reactions R5–R8:



The cycling time between OH and  $\text{HO}_2$  is only a few seconds, while the lifetime of  $\text{HO}_x$  is much longer (on the order of 30 min) (Jaeglé et al. 2001). [OH] and  $[\text{HO}_2]$ , therefore, are in a photochemical steady state under virtually any sunlit condition. [OH] is thus controlled not only by its production reactions, but by the production reactions for  $\text{HO}_2$ , the loss reactions of  $[\text{HO}_x]$  and the redistribution between [OH] and  $[\text{HO}_2]$  via reactions R5 to R8 (McKeen et al. 1997; Crawford et al. 1999; Jaeglé et al. 2001).  $[\text{HO}_x]$  is controlled only by its sources and sinks. The combination of R1 and R2 is one of the main  $\text{HO}_x$  sources, and  $\text{NO}_y$  is a major  $\text{HO}_x$  sink (Wennberg et al. 1998; Jaeglé et al. 2001; Hanisco et al. 2001). In this dataset,  $[\text{O}_3] \cdot [\text{H}_2\text{O}]$  showed no correlation with  $[\text{NO}_y]$  ( $r^2=0.17$ ). This lack of correlation is expected because  $[\text{H}_2\text{O}]$ ,  $[\text{O}_3]$ , and  $[\text{NO}_y]$  are independently determined by an air parcel's temperature history, photochemical history, and the combination of photochemical history and wet removal processes, respectively.  $[\text{HO}_x]$  showed little or no correlation with  $[\text{O}_3] \cdot [\text{H}_2\text{O}]$  ( $r^2=0.12$ ; data with  $\text{SZA} > 65^\circ$  are excluded due to their apparent correlation with the changing solar radiation or SZA) and  $1/[\text{NO}_y]$  ( $r^2=0.49$ ). This is not surprising since any possible single correlation between  $\text{HO}_x$  and one of its sources or sinks can easily be obscured by variations in other sources and sinks.  $[\text{HO}_x]$  did show a significant correlation with  $[\text{O}_3] \cdot [\text{H}_2\text{O}]/[\text{NO}_y]$  (Fig. 3,  $r^2=0.72$ ), consistent with the notion of  $[\text{O}_3] \cdot [\text{H}_2\text{O}]$  (via R1 and R2) and  $[\text{NO}_y]$  (via R9

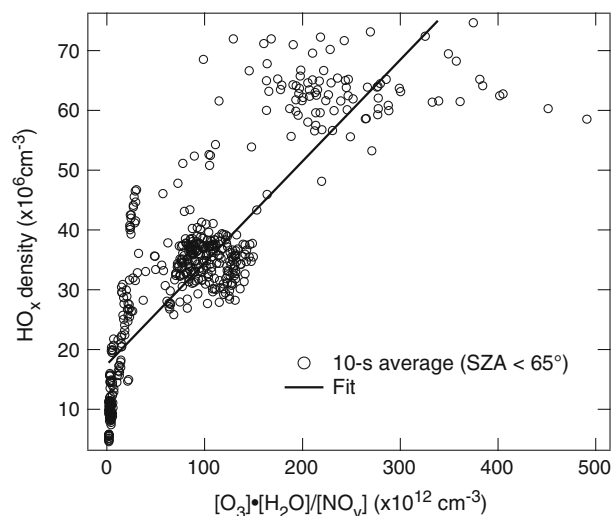


**Fig. 3** Correlation plot of  $\text{HO}_x$  density (10-s average) and  $[\text{O}_3]\cdot[\text{H}_2\text{O}]/[\text{NO}_y]$ . Data points with solar zenith angles greater than  $65^\circ$  are excluded to minimize the effect of changing solar radiation

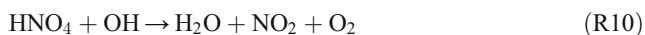
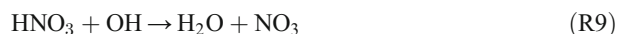
and R10) being a significant source and sink, respectively. This correlation can be seen in Fig. 2c and d, where at any SZA less than  $65^\circ$ , low  $[\text{HO}_x]$  corresponds to low  $[\text{O}_3]\cdot[\text{H}_2\text{O}]$  and high  $[\text{NO}_y]$ , and vice versa. Because neither  $[\text{O}_3]\cdot[\text{H}_2\text{O}]$  nor  $[\text{NO}_y]$  are the sole source and sink for  $[\text{HO}_x]$ , a tight correlation between  $[\text{HO}_x]$  and  $[\text{O}_3]\cdot[\text{H}_2\text{O}]/[\text{NO}_y]$  is not expected.

The theoretical  $[\text{HO}_2]$ -to- $[\text{OH}]$  ratio can be calculated using reactions R5–R8 and measured  $[\text{O}_3]$ ,  $[\text{CO}]$ ,  $[\text{NO}]$ , pressure, and temperature:

$$\frac{[\text{HO}_2]}{[\text{OH}]} = \frac{k_{\text{OH}+\text{CO}}[\text{CO}] + k_{\text{OH}+\text{O}_3}[\text{O}_3]}{k_{\text{HO}_2+\text{NO}}[\text{NO}] + k_{\text{HO}_2+\text{O}_3}[\text{O}_3]} \quad (2)$$

where  $k_x$  denotes the respective reaction rate. The calculated  $[\text{HO}_2]$ -to- $[\text{OH}]$  ratio is compared with measurements, expressed as a ratio of the calculated ratio to the measured ratio, in Fig. 4. As shown, the calculations generally agree with the measurements to within 30 %. The NO signal-to-noise ratio is low at extremely low and high SZAs (Fig. 2b), and hence results at SZA  $< 8.5^\circ$  and  $> 78^\circ$  are not included in the plot. The contribution of R6 is negligible and R7 dominates the  $\text{HO}_2$  reactions. The steady-state approximation used in deriving Eq. (2) is reasonably accurate even at the lowest  $[\text{NO}]$  values, in which case the  $\text{HO}_2$  self-reaction (R12) is still approximately a factor 3 slower than reactions R7 and R8.

Reactions involving  $\text{HNO}_3$  and  $\text{HNO}_4$ , significant components of  $\text{NO}_y$ , are sinks of  $\text{HO}_x$ . The key reactions are:



R7, R9, and R10 are a set of buffering reactions for OH when R9 and R10 are major sinks for  $\text{HO}_x$  and when NO is correlated with  $\text{HNO}_3$  and  $\text{HNO}_4$ : Higher  $[\text{HNO}_3]$  and  $[\text{HNO}_4]$  lead to lower  $[\text{HO}_x]$ , but the associated higher  $[\text{NO}]$  forces a lower  $[\text{HO}_2]$ -to- $[\text{OH}]$  ratio in the  $\text{HO}_x$  partitioning. An example where this buffering effect breaks down can be seen in the ER-2

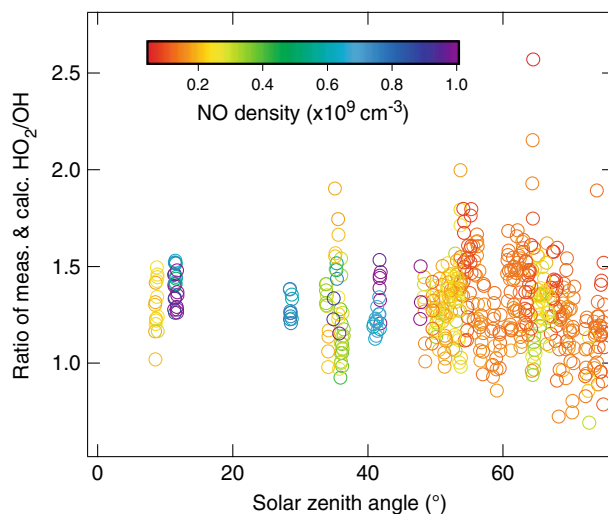


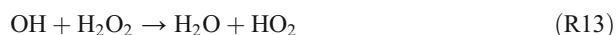
**Fig. 4** Ratio of 10-s averages of measured and calculated HO<sub>2</sub>-to-OH ratios are shown as a function of solar zenith angle (SZA)

plume sampling events (large black circles in Fig. 2); here NO produced by the ER-2 engine (Fahey et al. 1995) clearly forced [OH] out of its nominal relationship with SZA while [HO<sub>x</sub>] values show no apparent response to this additional [NO]. (Note that OH production may be enhanced by HONO in the ER-2 exhaust (Hanisco et al. 1997), but the photolysis of HONO is too slow to affect the [HO<sub>2</sub>]-to-[OH] ratio.) When NO<sub>y</sub> is too low to be the main HO<sub>x</sub> sink, this buffering effect will also break down.

When [NO<sub>y</sub>] is low, [HO<sub>x</sub>] is limited by the quadratic self-reactions:



and



and reactions with CH<sub>3</sub>OOH (Jaeglé et al. 2001). These self-reactions partially explain the relatively small changes in [HO<sub>x</sub>] when [O<sub>3</sub>] $\cdot$ [H<sub>2</sub>O] varies over 3 orders of magnitude. Another possible reason for the small HO<sub>x</sub> variations is additional, more constant HO<sub>x</sub> sources via ketone photochemistry (McKeen et al. 1997) and autocatalytic production through methane oxidation (Crawford et al. 1999; Jaeglé et al. 2001).

While [O<sub>3</sub>] and [H<sub>2</sub>O] show little effect on [OH], low [NO] and [NO<sub>y</sub>] conditions may lead to anomalously low [OH] due to the breakdown of the NO-HNO<sub>3</sub>-HNO<sub>4</sub> buffer. Under these conditions, while NO<sub>y</sub> is too low to be the major sink of HO<sub>x</sub>, the HO<sub>x</sub> values still are limited due to its self-reactions. While HO<sub>x</sub> values are self-limited, the low values of NO may not be able to recycle sufficient OH from HO<sub>2</sub> (R7). As shown in Fig. 2, very low [OH] values (more than a factor of 2 lower than the functional fit of Hanisco et al. (2001)) were observed during the STRAT mission (5°–10° SZA in Fig. 2a and b). These low [OH] values were associated with low [O<sub>3</sub>] (<2 $\times$ 10<sup>11</sup> cm<sup>-3</sup>), [NO] (<1 $\times$ 10<sup>8</sup> cm<sup>-3</sup>), and [NO<sub>y</sub>] (<2 $\times$ 10<sup>8</sup> cm<sup>-3</sup>). Note that the



corresponding  $[\text{HO}_x]$  (i.e.  $\text{HO}_2$ ) was actually at its highest within the STRAT dataset. In this case the recycling rate of  $\text{HO}_2$  back to OH was too slow to keep up with the loss of OH through reaction with  $\text{HO}_2$ , resulting in the decreased [OH]. This link between low [NO] and low [OH], if characteristic of air lifted to the TUT over the western Pacific warm pool via convection, will have important implications. The western Pacific warm pool is known to be a region of large-scale deep convection, which brings a large amount of  $\text{O}_3$ -poor air to the TUT. It appears that [NO] is also likely to be low in these air parcels both from limited STRAT data and the fact that lightning is rare in marine convection (Crawford et al. 1997; Christian et al. 2003; Cecil et al. 2012). These low values occur in a region where air is transported into stratosphere (Schoeberl et al. 2013). Low [OH] values may affect the breakdown rates of various ozone depleting species (Brioude et al. 2010). We note that [OH] may be enhanced in TUT air parcels originating from land-based convection, where lightning is common (Cecil et al. 2012).

#### 4 Conclusions

OH,  $\text{HO}_2$ , and other chemical species were measured in the TUT region during the STRAT aircraft campaign. While [OH] values show a robust relationship with SZA, they are essentially independent of  $[\text{O}_3]$  and  $[\text{H}_2\text{O}]$ . The majority of measured [OH] values, therefore, can be expressed using the simple formula (Eq. 1) reported by Hanisco et al. (2001) for stratospheric measurements.

The robust [OH]-SZA relationship is likely due to strong buffering. A well-known buffering mechanism (NO favoring OH within the partitioning of  $\text{HO}_x$ , and  $\text{HNO}_3$  and  $\text{HNO}_4$  limiting  $\text{HO}_x$  concentration) appears to play a role when  $\text{NO}_y$  is high. However, it is unclear that whether this mechanism alone is sufficient to account for the robust [OH]-SZA relationship.

Low-[OH] air parcels that fall well outside the [OH]-SZA relationship were encountered at times during Pacific tropical flights. These air masses are characterized by very low  $[\text{O}_3]$ , [NO], and  $[\text{NO}_y]$ . We postulate that the low  $[\text{NO}_y]$  conditions render the NO- $\text{HNO}_3$ - $\text{HNO}_4$  buffer ineffective, while low [NO] slows down the recycling of OH from  $\text{HO}_2$ , thus leading to low [OH] in these air parcels. This potential link between low [NO] and low [OH] has important consequences such as lowering the removal efficiency of surface pollutants over the west Pacific warm pool and allowing more efficient transport of very short-lived ozone-depleting substances and other compounds such as  $\text{SO}_2$  into the stratosphere.

**Acknowledgments** This work was supported by the NOAA Atmospheric Composition and Climate Program and the NOAA Health of the Atmosphere Program, the NASA Radiation Sciences Program, and the NASA Upper Atmosphere Research Program. We would like to thank the NASA ER-2 program for making the mission possible. We thank M. Rex and L. L. Pan for insightful discussions.

#### References

- Brioude, J., Portmann, R.W., Daniel, J.S., Cooper, O.R., Frost, G.J., Rosenlof, K.H., Granier, C., Ravishankara, A.R., Montzka, S.A., Stohl, A.: Variations in ozone depletion potentials of very short-lived substances with season and emission region. *Geophys. Res. Lett.* **37**, L19804 (2010). doi:10.1029/2010GL044856
- Cecil, D.J., et al.: Gridded lightning climatology from TRMM-LIS and OTD: dataset description. *Atmos. Res.* (2012). doi:10.1016/j.atmosres.2012.06.028
- Christian, H.J., et al.: Global frequency and distribution of lightning as observed from space by the Optical Transient Detector. *J. Geophys. Res.* **108**(D1), 4005 (2003). doi:10.1029/2002JD002347

- Crawford, J., et al.: Implications of large scale shifts in tropospheric  $\text{NO}_x$  levels in the remote tropical Pacific. *J. Geophys. Res.* **102**(D23), 28,447–28,468 (1997)
- Crawford, J., et al.: Assessment of upper tropospheric  $\text{HO}_x$  sources over the tropical Pacific based on NASA GTE/PEM data: net effect on  $\text{HO}_x$  and other photochemical parameters. *J. Geophys. Res.* **104**(D13), 16255–16273 (1999). doi:[10.1029/1999JD900106](https://doi.org/10.1029/1999JD900106)
- Denning, R.F., Guidero, S.L., Parks, G.S., Gary, B.L.: Instrument description of the airborne microwave temperature profiler. *J. Geophys. Res.* **94**, 16,757–16,765 (1989)
- Fahey, D.W., et al.: In situ observations in aircraft exhaust plumes in the lower stratosphere at midlatitudes. *J. Geophys. Res.* **100**, 3065–3074 (1995)
- Fahey, D.W., et al.: In situ observations of  $\text{NO}_y$ ,  $\text{O}_3$ , and the  $\text{NO}_y/\text{O}_3$  ratio in the lower stratosphere. *Geophys. Res. Lett.* **23**, 1653–1656 (1996)
- Folkens, I., Bernath, P., Boone, C., Donner, L.J., Eldering, A., Lesins, G., Martin, R.V., Sinnhuber, B.-M., Walker, K.: Testing convective parameterizations with tropical measurements of  $\text{HNO}_3$ ,  $\text{CO}$ ,  $\text{H}_2\text{O}$ , and  $\text{O}_3$ : implications for the water vapor budget. *J. Geophys. Res.* **111**, D23304 (2006). doi:[10.1029/2006JD007325](https://doi.org/10.1029/2006JD007325)
- Gao, R.S., et al.: Partitioning of the reactive nitrogen reservoir in the lower stratosphere of the southern hemisphere: Observations and modeling. *J. Geophys. Res.* **102**, 3935–3949 (1997)
- Hanisco, T.F., et al.: The role of  $\text{HO}_x$  in super- and subsonic aircraft exhaust plumes. *Geophys. Res. Lett.* **24**, 65–68 (1997)
- Hanisco, T.F., et al.: Sources, sinks, and the distribution of OH in the lower stratosphere. *J. Phys. Chem. A* **105**, 1543–1553 (2001)
- Jaeglé, L., Jacob, D.J., Brune, W.H., Wennberg, P.O.: Chemistry of  $\text{HO}_x$  radicals in the upper troposphere. *Atmos. Environ.* **35**, 469–489 (2001)
- Kley, D., Crutzen, P.J., Smit, H.G.J., Vomel, H., Oltmans, S.J., Grassl, H., Ramanathan, V.: Observations of near-zero ozone concentrations over the convective pacific: effects on air chemistry. *Science* **274**, 230–233 (1996)
- McKeen, S.A., Gierczak, T., Burkholder, J.B., Wennberg, P.O., Hanisco, T.F., Keim, E.R., Gao, R.S., Liu, S.C., Ravishankara, A.R., Fahey, D.W.: The photochemistry of acetone in the upper troposphere: a source of odd-hydrogen radicals. *Geophys. Res. Lett.* **24**, 3177–3180 (1997)
- Montzka, S.A., Krol, M., Dlugokencky, E., Hall, B., Jöckel, P., Lelieveld, J.: Small interannual variability of global atmospheric hydroxyl. *Science* **331**, 67–69 (2011)
- Newell, R.E., Gould-Stewart, S.: A stratospheric fountain? *J. Atmos. Sci.* **38**, 2789–2796 (1981)
- Proffitt, M.H., McLaughlin, R.J.: Fast-response dual-beam UV-absorption ozone photometer suitable for use on stratospheric balloons. *Rev. Sci. Instrum.* **54**, 1719–1728 (1983)
- Rae, J.G.L., Johnson, C.E., Bellouin, N., Boucher, O., Haywood, J.M., Jones, A.: Sensitivity of global sulphate aerosol production to changes in oxidant concentrations and climate. *J. Geophys. Res.* **112**, D10312 (2007). doi:[10.1029/2006JD007826](https://doi.org/10.1029/2006JD007826)
- Rohrer, F., Berresheim, H.: Strong correlation between levels of tropospheric hydroxyl radicals and solar ultraviolet radiation. *Nature* **442**, 184–187 (2006). doi:[10.1038/nature04924](https://doi.org/10.1038/nature04924)
- Schoeberl, M.R., Dessler, A.E., Wang, T.: Modeling upper tropospheric and lower stratospheric water vapor anomalies. *Atmos. Chem. Phys.* **13**, 7783–7793 (2013). doi:[10.5194/acp-13-7783-2013](https://doi.org/10.5194/acp-13-7783-2013)
- Scott, S.G., Bui, T.P., Chan, K.R., Bowen, S.W.: The meteorological measurement system on the NASA ER-2 aircraft. *J. Atmos. Ocean. Technol.* **7**, 525–540 (1990)
- Skamarock, W.C., Dye, J.E., Defer, E., Barth, M.C., Stith, J.L., Ridley, B.A.: Observational- and modeling-based budget of lightning-produced  $\text{NO}_x$  in a continental thunderstorm. *J. Geophys. Res.* **108**, D10 (2003). doi:[10.1029/2002JD002163](https://doi.org/10.1029/2002JD002163)
- Webster, C.R., May, R.D., Trimble, C.A., Chave, R.G., Kendall, J.: Aircraft (ER-2) laser infrared absorption spectrometer (ALIAS) for *in-situ* stratospheric measurements of HCl,  $\text{N}_2\text{O}$ ,  $\text{CH}_4$ ,  $\text{NO}_2$ , and  $\text{HNO}_3$ . *Appl. Opt.* **33**, 454–472 (1994)
- Weinstock, E.M., et al.: New fast-response photofragment fluorescence hygrometer for use on the NASA ER-2 and the Perseus remotely piloted aircraft. *Rev. Sci. Instrum.* **65**(11), 3544–3554 (1994)
- Weisenstein, D.K., Yue, G.K., Ko, M.K.W., Sze, N.-D., Rodriguez, J.M., Scott, C.J.: A two-dimensional model of sulfur species and aerosol. *J. Geophys. Res.* **102**(D11), 13019–13035 (1997)
- Wennberg, P.O., Cohen, R.C., Hazen, N.L., Lapson, L.B., Allen, N.T., Hanisco, T.F., Oliver, J.F., Lanham, N.W., Demusz, J.N., Anderson, J.G.: Aircraft-borne, laser-induced fluorescence instrument for the *in situ* detection of hydroxyl and hydroperoxyl radicals. *Rev. Sci. Instrum.* **65**, 1858–1876 (1994a). doi:[10.1063/1.1144835](https://doi.org/10.1063/1.1144835)
- Wennberg, P.O., et al.: Removal of stratospheric  $\text{O}_3$  by radicals: in situ measurements of OH,  $\text{HO}_2$ , NO,  $\text{NO}_2$ , ClO, and BrO. *Science* **266**, 398–404 (1994b)
- Wennberg, P.O., et al.: Hydrogen radicals, nitrogen radicals, and the production of  $\text{O}_3$  in the upper troposphere. *Science* **279**, 49–53 (1998)